



Conformational Dynamics of 4-Aryl-1,4-Dihydropyridine Calcium Channel Antagonists. 1. Quantitation of C4-C1' Bond Rotational Barriers

Robert B. Palmer and Niels H. Andersen*

Department of Chemistry, University of Washington, Seattle, WA 98195

Abstract: The solution state dynamics of six substituted 4-aryl-1,4-dihydropyridine calcium channel antagonist analogs were studied using saturation transfer, difference NOE and variable temperature NMR spectroscopy. Thermodynamic activation parameters for aryl ring rotation were determined for all six compounds from linear Eyring plots which span four orders of magnitude. The barrier to rotation about the ring juncture was also calculated at the AM1 level and these calculations correctly predict the general magnitude, though not the specific barriers, to rotation. The asymmetrically substituted compound, 1,4-dihydro-2,6-dimethyl-4-(2'-chloro-6'-methylphenyl)-3,5-pyridine-dicarboxylic acid dimethyl ester (**2a**), showed a rotameric preference of 1.7:1 by NMR for having the aryl methyl group *syn* to the C4H of the dihydropyridine ring; AM1 correctly predicts this preference but overestimates its magnitude. In the crystal state, the rotameric ratio appears to be nearer 1:1.

Copyright © 1996 Elsevier Science Ltd

Introduction

4-aryl-1,4-dihydropyridines (aryl-DHP's) such as nifedipine (**4a**) (Figure 1) are calcium channel antagonists that are used clinically for the treatment of angina and hypertension.¹ All pharmacologically potent aryl-DHP calcium channel antagonists have asymmetrically substituted 4-aryl rings.²⁻⁴ When the DHP ring is replaced by an asymmetric mimic, the C4 enantiospecificity of biopotency is very high.⁵⁻⁶ These structure-activity features argue for a distinct rotameric preference about the C4-C1' bond in the receptor bound state. As a result, considerable speculation and experimentation has been aimed at deriving the rotameric preference and barrier to this rotation.⁷⁻⁸ The two low energy rotameric conformations place the ring planes orthogonal to one another. The rotamers are designated *syn*- (with C2' substituent closest to the C4H) and *anti*- (with the 2' substituent facing away from the C4H) (Figure 2). Crystallographic examination has shed some light on the solid state rotameric preferences about the ring juncture but the question of the solution state conformation remains largely unanswered.⁹⁻¹⁴

Until quite recently, it was assumed that the barrier to aryl ring rotation was large and analogs were thought to have a distinct frozen rotameric form.¹⁵ This notion was supported by calculations that predicted very large rotational barriers¹⁶ and substantial rotameric preferences (3-4 kcal for the geometry with the 2'-aryl substituent *syn* to the C4H of a mono substituted aryl ring). The conclusions from experimental studies, however, stand in distinct contrast to those calculations and assumptions. NMR studies by Rovnyak *et al.* showed rapid rotation at ambient temperature for aryl DHP's with one *ortho*- substituent and a difference in energy between *syn* and *anti* rotamers

* To whom correspondence should be addressed

of less than 1 kcal based on NOE studies and that out of the 6 compounds they studied, the small rotameric preference in five was for the *ortho* substituent in the *syn* geometry.¹⁷ It is now clear that in order to "freeze out" these rotations on the NMR time scale at the attainable temperatures, there must be substantial steric bulk in at least one, if not both, of the aryl positions *ortho*- to the DHP ring.

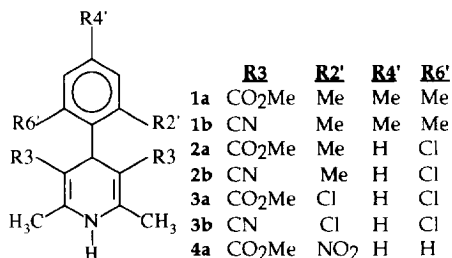


Figure 1. DHP's examined in this study.

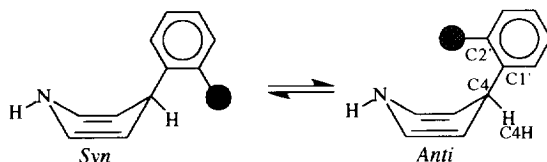


Figure 2. Definitions of *syn* and *anti* rotamers

The results obtained by Goldmann and Geiger in 1984 for the 2',4',6'-trimethyl compound, **1a**, showed that the 4-aryl group was rotating about the ring juncture between the phenyl and DHP rings (henceforth, called the C4-C1' bond).¹⁸ The authors reported that the rotameric exchange sites could be separated at low temperature in the NMR and estimated the barrier for this rotational process at *circa* 51 kJ/mol.¹⁸ Here we report a thorough analysis of this compound's behavior as well as a comparative study with five other analogues. The asymmetrically substituted species (**2a,b**) were included to probe the question of rotameric preference. In each case, we expected to be able to freeze out the rotamers at practically attainable temperatures.

Chemical Syntheses

The Hantzsch pyridine synthesis, with the omission of the final oxidation to the pyridine (Figure 3), was used throughout. This is known to give low yields when bulky 2',6' substituents are present.¹⁸⁻¹⁹ The synthesis of the requisite *ortho*-substituted aryl aldehydes can also be problematic. Compounds **2a** and **3a** were prepared *via* a standard Hantzsch process while compound **1a** was synthesized by first condensing 2,4,6-trimethylbenzaldehyde in a Knoevenagel manner with methylacetoacetate to form the benzylidene acetate. This product was then converted to dihydropyridine **1a** using 2-methylaminocrotonate.

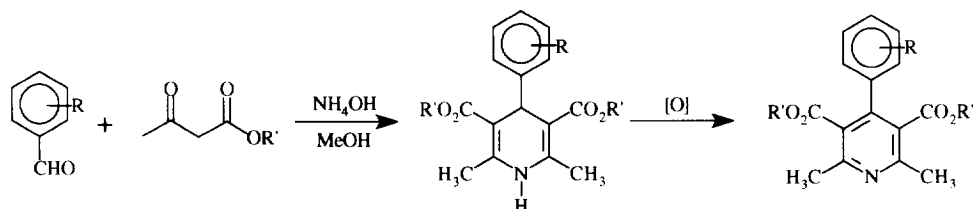


Figure 3. The Hantzsch pyridine synthesis

Table 1. Analytical data for compounds

	<u>mp</u>	<u>Yield</u>	<u>HRMS</u>	<u>¹H NMR</u>
1a	188-190°C (lit. 180-182°C) ¹⁸	9%	C ₂₀ H ₂₅ NO ₄ Calc'd: 343.1783 Found: 343.1784	δ 6.73 (s, 2H), 5.53 (s, 1H, C4H), 5.40 (bs, 1H, NH), 3.50 (s, 6H), 2.39 (s, 6H), 2.18 (s, 3H), 2.17 (s, 6H)
2a	208-211°C	1.5%	C ₁₈ H ₂₀ NO ₄ Cl Calc'd: 349.1081 Found: 349.1079	δ 7.15 (bd, 1H, J=7.5 Hz, H3'), 6.98 (bd, 1H, J=7.5 Hz, H5'), 6.94 (overlapping dd, 1H, J=7.5 Hz, H4'), 5.72 (bs, 1H, NH), 5.57 (s, 1H, C4H), 3.52 (s, 6H), 2.57 (s, 3H), 2.21 (s, 6H)
2b	240-242°C	68%	C ₁₆ H ₁₄ N ₃ Cl Calc'd: 283.0876 Found: 283.0876	δ 7.29 (dd, 1H, J=7.6 Hz, J=2.4 Hz), 7.15 (bd, 1H, J=7.6 Hz), 7.12 (bd, 1H, J=6.9 Hz), 6.04 (bs, 1H, NH), 5.70-5.15 (bs, (skewed with a shoulder for the minor conformer) 1H, C4H), 2.48-2.40 (bs, (skewed with a shoulder for the minor conformer) 3H), 2.04 (s, 6H).
3b	224-226°C	56%	C ₁₅ H ₁₁ N ₃ Cl ₂ Calc'd: 303.0330 Found: 303.0326	δ 7.38 (bd, 2H, J=8.0 Hz), 7.21 (overlapping dd, 1H, J=8.1 Hz), 6.07 (bs, 1H, NH), 5.67 (s, 1H, C4H), 2.06 (s, 6H).

Compounds **1b** and **3a** were received as gifts from Dr. S. D. Kimball of Bristol-Myers Squibb, Princeton, New Jersey.

The 3,5-dinitrile DHP's, **1b**, **2b** and **3b**, were synthesized by the method reported by Loev *et al.* in which the appropriately substituted aryl aldehyde was refluxed with two to three equivalents of 3-aminocrotonitrile in glacial acetic acid.²⁰ After a 1-2 hour reflux, the crude dihydropyridine precipitated from the reaction mixture.

Purification of the dihydropyridines was accomplished by rapid chromatography on silica gel (if left on the silica for an extended period, oxidation to the pyridine occurs) followed by recrystallization from either an anhydrous alcohol or a mixture of an absolute alcohol and acetonitrile. The compounds were then dried under vacuum and rinsed with ice-cold diethyl ether. Analytical data are contained in Table 1. Further synthetic details are given in a Ph. D. dissertation.²¹

Results and Discussion

Within the variable temperature NMR spectra of the DHP's, examined herein, there are a variety of temperature dependent spectral changes that are manifestations of dynamic events. The focus of this paper is the so-called "principal dynamic" - C4-C1' bond rotation (Figure 2). Discussion of the other dynamic possibilities is deferred elsewhere.²¹⁻²² When rotation about the C4-C1' bond slows such that individual conformers can be detected, the first notable change is at the 2' and 6' substituents (methyl groups in the case of **1a**), as previously shown by Goldmann and Geiger.¹⁸ The *anti*-methyl is located directly over (*i.e.* in the shielding cone of) the DHP ring *anti* to C4H while the other methyl group is *syn* to C4H. Additionally, the 3' and 5' aromatic signals become nonequivalent for the same reasons but the difference in chemical shift between them is less dramatic. This is illustrated (Figure 4) by a study of the 2',6'-dichlorophenyl species (**3a**). No change is observed in the signal of 4' substituent as it lies on the axis of rotation. The symmetry of the mesityl group of **1a** dictates that the two "rotamers" are identical and equally populated.

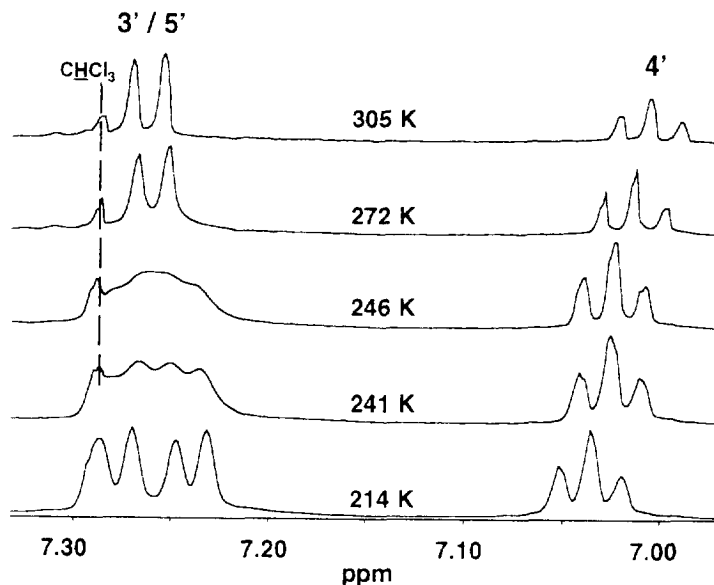


Figure 4. The aryl region of the variable temperature ^1H NMR spectrum of the 2',6'-dichlorophenyl-3,5-diester DHP (**3a**). The doublet corresponding to the 3'/5' aryl protons at 305 K splits into two separate doublets as shown at 214 K. The 4' aryl signal shows only a temperature gradient manifested by a downfield shift with decreasing temperature.

Therefore, except for the similar splitting seen in the 3' and 5' aromatics, no additional changes are found elsewhere in the spectra. However, in the case of an asymmetrically substituted aryl ring, such as the 2'-chloro-6'-methylphenyl rings in **2a** and **2b**, the rotamers are distinctly different despite the size similarity between a chlorine and a methyl group. In these cases, the signals for C4H, N1H, C2/C6 methyls and possibly the ester signals could split and show signals whose integrals reflect relative rotameric populations. Examination of the temperature dependence of the 6'-methyl group in the 2'-chloro-6'-methyl DHP (**2a**) in Figure 5, reveals that the two low temperature signals are inequivalent in size and that the population weighted average signal at high temperature lies significantly closer to the higher population site.

Beginning with the 3,5-dimethoxycarbonyl series, for compounds **1a** and **2a**, the rate of rotation about the C4-C1' bond could be determined using ^1H NMR by the broadening, and subsequent splitting, of the *ortho* methyl signal with cooling. At 500 MHz, coalescence temperatures (T_c) of 261 ± 5 and 266 ± 8 K were observed for **1a** and **2a** respectively. In the case of **3a**, only the 3'/5' *meta* proton signal could be used for this purpose and had a T_c of 249 ± 3 K. This was also used as a secondary probe for **1a** ($T_c = 238 \pm 3$ K).

The 3,5-dinitrile substituted compounds, **1b**, **2b** and **3b**, behaved somewhat differently than their 3,5-diester relatives. C4-C1' rotation in **1b** was already "frozen-out" at room temperature in the methyl signals. However, it was not visible in the 3'/5' aryl signals even at the low temperature extreme. Warming the sample caused the signals for the two *ortho*-methyl groups to coalesce

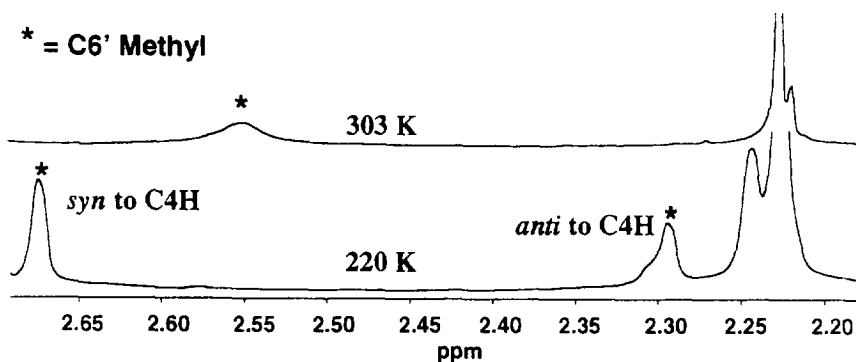


Figure 5. The C6' methyl group of the 2'-chloro-6'-methyl compound, **2a**, at 303 K and 220 K. Note the unequal rotameric populations as is evident from the high temperature population weighted average shift as well as the signal intensities at the low temperature.

($T_c = 331 \pm 5$ K). Similarly, the ^1H spectrum for the 2'-chloro-6'-methyl compound (**2b**) had a broad signal with a smaller broad signal merging with it on the upfield side at room temperature. These two signals correspond to the 6'-methyl group of the two unequally populated rotamers of **2b** (illustrated in Figure 6). Therefore, only slight cooling to 290 K was required to freeze-out the rotation ($T_c = 331 \pm 8$ K).

Determination of T_c was more complicated for compound **3b**. Not only was there a separation of signals from the freezing out of the rotation but the signals of the two rotamers have different temperature gradients. This was evident from the separation of the 3'/5' aromatic doublet into two doublets as the temperature was lowered followed by the apparent re-collapsing of the signals into "one doublet" with an additional temperature decrease. The loss of the rotamer

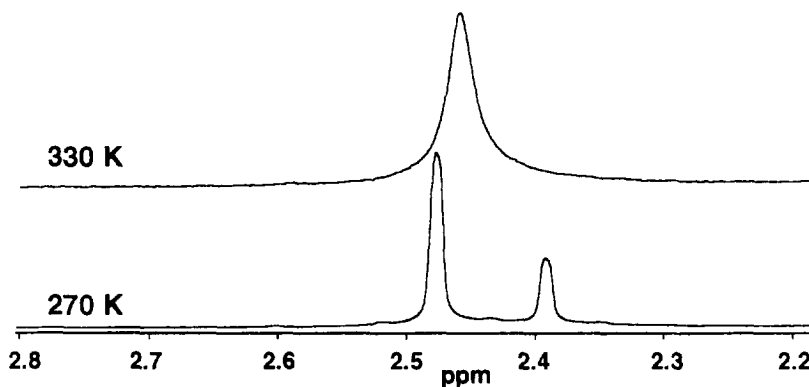


Figure 6. The methyl region of the variable temperature ^1H NMR spectrum of the 2'-chloro-6'-methylphenyl-3,5-dinitrile DHP (**2b**). The broad signal corresponding to the 2'/6' methyls at 330 K splits into two separate signals as shown at 270 K.

separation on further cooling cannot be attributed to temperature-dependent line broadening since the linewidth of the 3'/5' aromatic doublet at the low temperature extreme was less than that of a single line of the 4' aromatic signal at the same temperature. In order to derive $\Delta\nu$ at T_C for the rotational process, the temperature gradients must be considered. To do this, $\Delta\nu$ was measured for several different temperatures, all of which were below the estimated T_C of 298 K. This was plotted against absolute temperature (Figure 7) and $\Delta\nu$ at 298 K was extrapolated from the resulting linear graph. This method yielded $\Delta\nu=5.17$ Hz at 298 K, which is a substantial extrapolation.

The initial estimates of rotational barriers were based on equation (1), which assumes equal populations of rotamers.²³

$$\Delta G^\ddagger = 19.14 T_C (9.97 + \log(T_C/\Delta\nu)) \text{ J/mol} \quad (1)$$

In the case of the asymmetric 3,5-diester compound (**2a**), a 1.5:1 ratio of rotamers was observed in solution by integration. The analogous 3,5-dinitrile, **2b**, however, has rotameric population ratio of 4.1:1 by integration. The unequal populations introduce error into the energy barrier estimations using equation (1). To reflect the uncertainties associated with unequal population, the T_C error

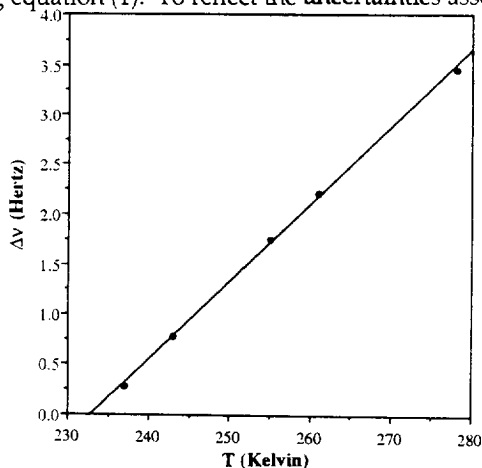


Figure 7. Plot of $\Delta\delta$ versus temperature for the 3'/5' aryl protons of the 2',6'-dichloro-3,5-dinitrile DHP (**3b**). This graph was used to correct for the observed temperature gradient in the signals and to extrapolate $\Delta\delta$ to T_C (298 K).

estimates are taken as 150% of the errors in T_C 's for cases with equally populated exchange sites. The ΔG^\ddagger error estimate follows from estimated errors in determining T_C and $\Delta\nu$ (at T_C). To obtain $\Delta\nu(T_C)$, $\Delta\nu_{obs}$ was plotted over the region from 10 to 90 K below T_C for all systems studied. The errors in $\Delta\nu(T_C)$ were estimated as the difference in chemical shift at the highest "observed" temperature point on the $\Delta\nu$ versus T plot and the extrapolated value of $\Delta\nu$ at T_C . The errors in ΔG^\ddagger were estimated by using half of the difference between the ΔG^\ddagger derived from the high T_C and low $\Delta\nu$ and the ΔG^\ddagger derived from the low T_C and high $\Delta\nu$ estimate for each compound. The results are tabulated in Table 2.

It is clear that the 3,5-dinitrile compounds have smaller differences in chemical shift for the rotameric sites than the analogous diesters, yet the temperatures of coalescence are higher in the dinitrile series: the dinitriles have notably higher rotational barriers than the diesters. The data suggest a slight increase in barrier with the replacement of a methyl group with a chlorine. The largest errors reported are for the two asymmetric compounds, **2a** and **2b**. The greater uncertainty

Table 2. Estimates of rotational barriers for phenyl DHP's based on equation (1).

	Probe	$\Delta\nu$ (Hz)	T_C (K)	ΔG^\ddagger (kJ/mol)
1a	^{13}C -2',6'	226	265	50.9
1a	CH_3	164.8 ± 6.2	261 ± 5	50.8 ± 1.1
1a	Aryl-H	9.6 ± 1.6	238 ± 3	51.8 ± 1.0
1a	^{13}C -3',5'	7.7	235	51.5
1b	CH_3	39.4 ± 1.6	331 ± 5	69.0 ± 1.2
2a	CH_3	178.3 ± 6.2	266 ± 8	51.6 ± 1.7
2b	CH_3	35.4 ± 2.1	331 ± 8	69.3 ± 1.9
3a	^{13}C -2',6'	221	280	54.0
3a	^{13}C -3',5'	13.6	250	53.8
3a	Aryl-H	15.7 ± 0.8	249 ± 3	53.2 ± 0.8
3b	Aryl-H	5.2 ± 1.8	298 ± 3	66.9 ± 1.6

in these determinations are primarily a result of the unequal populations of sites. This inequality makes accurate determination of T_C very difficult and therefore increases the error in ΔG^\ddagger .

The expanded chemical shift range and greater number of signals of ^{13}C NMR spectroscopy makes it a logical choice for confirmation of the proton data at very low temperatures. Variable temperature ^{13}C NMR spectroscopy was employed to examine the 3,5-diester compounds **1a**, **2a** and **3a**. Once again, rotation about the C4-C1' bond was the principal dynamic isolated by the separation of the phenyl signals at low temperature. For both **1a** and **3a**, the *ortho* and *meta* aromatic carbons are well-resolved into rotameric sites at low temperatures. The barriers were estimated using equation (1). These values are in excellent agreement with the analogous barrier estimates based on the ^1H NMR data (see Table 2). The low temperature spectra of the 2'-chloro-6'-methyl-3,5-diester compound (**2a**) showed similar resolutions but were not of sufficient quality to estimate ΔG^\ddagger , but the T_C estimates were in accord with those derived from the ^1H NMR data.

The ΔG^\ddagger determinations for compound **1a** suggest a small positive entropy change associated with the ring rotation. The rates of rotation near the coalescence temperatures of the 2',4',6'-trimethylphenyl compound, **1a**, and the 2',6'-dichlorophenyl compound, **3a**, were obtained by complete lineshape analysis. Due to chemical shift overlap, only the downfield methyl signal was analyzed closely for peakshape in the case of **1a**. Eyring plots were constructed based on the lineshape analysis and yielded an initial set of thermodynamic parameters (which appear as part of Table 3). This analysis indicated a small negative ΔS^\ddagger .

Rotational Rate Determination

In order to extend the temperature range over which rotation rates were measured, a standard transient difference NOE protocol was employed for inversion transfer experiments.²⁴ This allowed measurement of the rotation rates directly at 213 K for the diester compounds and at 273 - 278 K for the dinitrile compounds - at least 25°C below the coalescence temperatures. Figure 8 shows the magnetization transfer (from one 2'/6'-methyl site to the other) rate determination for the 2',4',6'-trimethyl compound, **1a**. The 2'-chloro-6'-methyl-3,5-diester compound (**2a**) gave a comparably precise determination. The rates were $2.78 \pm 0.40 \text{ sec}^{-1}$ (**1a**), $1.10 \pm 0.53 \text{ sec}^{-1}$ (**2a**, major

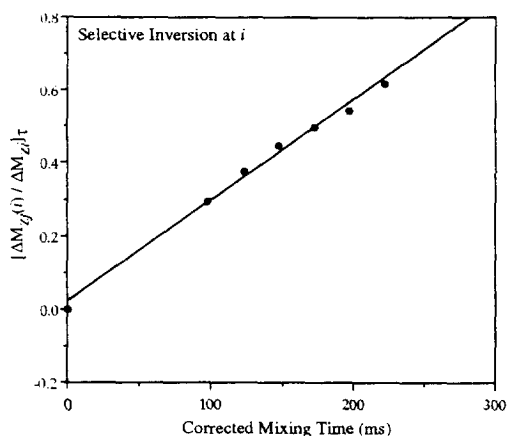


Figure 8. Magnetization transfer rate determination for the 2',4',6'-trimethylphenyl-3,5-diester DHP (**1a**) at 213 K. The spectra were collected directly as difference spectra and recorded as absolute intensities. Normalization was achieved by dividing the intensity of the non-irradiated peak by the intensity of the irradiated peak at each mixing time to give 'residual-driver-normalized NOEs'. By plotting this NOE intensity *versus* the mixing time (corrected for transfer during irradiation, see NMR methods), a linear plot is obtained for mixing times ≤ 250 ms. The slope of this plot is the rate at which inversion transfer occurs at this temperature. Since the only mechanism for magnetization transfer in these systems is by the physical re-orientation of atoms from a rotation, the transfer rate is the rate of rotation.

to minor) and $1.86 \pm 0.26 \text{ sec}^{-1}$ (**2a**, minor to major) - the latter corresponding to an equilibrium ratio of 1.7:1 at 213 K, in excellent accord with the 1.5:1 ratio observed by peak integration. For compounds **1b** and **2b**, the determined rates were $1.32 \pm 0.48 \text{ sec}^{-1}$ (**1b**), $0.53 \pm 0.32 \text{ sec}^{-1}$ (**2b**, major to minor) and $1.74 \pm 0.42 \text{ sec}^{-1}$ (**2b**, minor to major) - the latter corresponding to an equilibrium ratio of 3.3:1.

In several cases, poor resolution of signals for the individual sites precluded full selectivity of inversion. The rate determination ($2.38 \pm 0.63 \text{ sec}^{-1}$ at 213 K) for **3a** is less accurate but still useful ($\Delta\delta_{\text{syn/anti}} = 0.039 \text{ ppm}$, 18.50 Hz at 11.7 T). The determination of the rotational rate in **3b** was not possible for the same reason ($\Delta\delta_{\text{syn/anti}} = 0.010 \text{ ppm}$, 5.17 Hz at 11.7 T).

Additional rate estimates at temperatures far greater than the coalescence temperature, were added to the Eyring plots from measurements of the exchange induced line broadening and by estimation of k at the coalescence temperature.²³ Manual measurements of line broadening were used to construct an Eyring plot for the rotamerically unequally populated 2'-chloro-6'-methyl-3,5-diester compound (**2a**). The resulting Eyring plots are, in the best cases, linear over nearly four orders of magnitude (see, for example, Figure 9) and from them, thermodynamic activation parameters were determined. Eyring plots for **1b** and **2b** were constructed using the measured line broadening at and above T_c and inversion transfer at the lower temperatures. The resulting thermodynamic parameters are collected in Table 3. The Gibbs free energies calculated for T_c using the derived enthalpy and entropy terms correlated well (typically, $\pm 1 \text{ kJ/mole}$ or better) with the estimates of ΔG^\ddagger from equation (1) (Table 2). The observed 1.7:1 ratio of rotamers in **2a** as determined using relative rates (1.5:1 as determined by integration) and the rotameric ratios of **2b** (3.3:1 by relative rates and 4.1:1 by integration) serve to validate the exchange rate measurement protocol used. In both cases, the equilibrium favors the rotamer with the more downfield ArCH_3 .

The ΔG^\ddagger 's for the diester series increase in the order **1a** < **2a** < **3a**. The derived enthalpies for the same compounds do not follow this trend and increase as **1a** < **3a** < **2a**. Clearly, the difference in trends resides in the less well-determined entropic terms; the error in the $T\Delta S^\ddagger$ term is

Table 3. Estimates of rotational barriers for phenyl DHP's based on Eyring plots. The italicized numbers represent values obtained from Eyring plots constructed based on line shape analysis only.

	ΔH^\ddagger (<u><i>kJ/mol</i></u>)	ΔS^\ddagger (<u><i>J/K mol</i></u>)	ΔG^\ddagger (at T_c) (<u><i>kJ/mol</i></u>)
1a	47.7±5.8	-16±26	51.9±1.1 (at 262 K)
1a	56.6	-20	51.3
1b	59.3±10.5	-27±35	68.3±1.9 (at 333 K)
2a	50.0±7.0	-8±32	52.2±1.7 (at 275 K)
2b	58.7±11.6	-24±42	66.8±1.6 (at 337 K)
3a	49.7±8.6	-10±36	52.4±0.8 (at 270 K)
3a	63.9	-46	52.3

conservatively estimated as 6 kJ/mol or greater. Since we have erred on the side of error overestimation, we will make some use of the values in Table 3. A statement by Binsch and Kessler puts this in perspective nicely:²⁵ "Although DNMR spectroscopy is also suited for quantitative determination of activation enthalpies and entropies, experience shows that activation entropies of

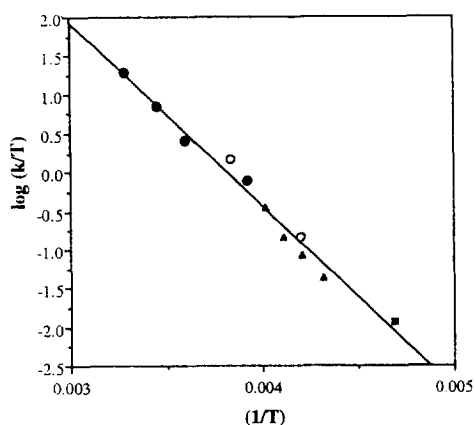


Figure 9. A typical Eyring plot (this one for the 2',4',6'-trimethylphenyl-3,5-dimethylester DHP (**1a**)) showing linearity over nearly four orders of magnitude. The saturation transfer point (filled square) was obtained using a standard difference NOE protocol at 213 K with "normalized" the peak intensities. Lineshape analysis (filled triangles) was used in the region close to the coalescence temperature. Points well above the coalescence temperature (for both aryl-methyl and aryl-hydrogen signals) were obtained using a manual measurement of linewidth due to exchange broadening (filled circles). This was accomplished by comparing the full width at half maximum of a non-exchanging peak to a the full width at half maximum of an exchanging peak at the same temperature. The difference between these two peak widths in Hertz is then attributed to exchange broadening. At rapid exchange and essentially equal populations, the rate of exchange, k , can be estimated as $k = \Delta\epsilon\pi$. The open circles on the plot represent points in which k was estimated at the respective coalescence temperatures by the relationship $k = \pi\Delta\nu/2^{1/2}$. These points are not included in the regression fit as the coalescence temperatures are the least well determined values.

an accuracy indispensable for a meaningful chemical interpretation are no longer obtained routinely."

Turning to the 3,5-dinitrile series, and using the ΔG^\ddagger exclusively from Table 2, the ΔG^\ddagger 's follow a different trend (**3b** < **1b** ~ **2b**) than their diester counterparts. In Table 3, both the entropy and enthalpy of **1b** are greater than those terms for **2b**. The entropic terms for the dinitrile series are also negative but appear to be larger in absolute value than those for the diester series. On balance,

the entropy terms tend to be small and negative for both series.

It is clear that in the cases of the 2'-chloro-6'-methyl analogues, **2a** and **2b**, an unequal rotameric population distribution exists (Figures 5 and 6). Therefore, it was important to determine which rotamer was favored. Even in the symmetric cases, it is desirable to know which signal corresponds to which non-equivalent site. Nuclear Overhauser Effect (NOE) experiments provide an unequivocal assignment. On average, a distance of 2.6 Å exists between a methyl group and C4H in a *syn* disposition and 4.1 Å from a methyl group *anti* to C4H, in the X-ray structures. Since the upper limit of utility of the magnetization transfer in an NOE experiment is about 4.5 Å, clearly a *syn* methyl will have a strong NOE from C4H while an *anti* methyl NOE from C4H will be very weak or undetectable.

The necessary NOE experiments were performed and showed clearly that the more downfield of the rotameric methyl signals in the 2',4',6'-trimethyl species (**1a** and **1b**), and in the 2'-chloro-6'-methyl species (**2a** and **2b**) corresponded to the *syn* position, leaving the more upfield to be assigned as the *anti* methyl. All NOE's were further confirmed by irradiating the methyl signals and looking for those that transferred magnetization to the C4H. This had an additional benefit in that the irradiation of the 2'/6'-methyl (which will then have an *anti/syn* assignment) will also lead to NOE's at the 3' and 5' aromatic protons. In this way, it was also confirmed in the 2',4',6'-trimethyl species (**1a** and **1b**) that the more downfield of the aromatic rotameric pair corresponded to the *syn* position and the more upfield to the *anti* position (*i.e.* located in the shielding cone of the DHP π -system). The analysis of the 2'-chloro-6'-methyl species (**2a** and **2b**) was analogous though slightly more complicated. The 2',6'-dichloro compounds (**3b** and **3a**), however, had to be assigned by analogy as no diagnostic NOE's were available.

Comparisons with Computational Barriers and Conformational Preferences

Experimental results rely on the ability to synthesize the compounds and run the experiments which is time-consuming and expensive. The ability to computationally model these experiments is certainly appealing. With the data pool established in this study, we believe an assessment of the usefulness of calculations is feasible.

There is disagreement in the literature regarding calculated barriers to ring juncture rotation in DHP's. For example, Natale *et al.* report a rotational barrier for a 3,5-dimethylisoxazolyl DHP of ~9 kcal/mol.²⁶ Holtje and Marrar used MNDO optimized geometries to conclude a rotameric preference with the C2' substituent *syn* to C4H was favored by 3-4 kcal/mol¹⁵ but Rovnyak *et al.* concluded on the basis of AM1 calculations that there was little intrinsic difference between *syn* and *anti* rotamers (for 2'-halo species).¹⁴ The results of Natale²⁶ and Rovnyak¹⁴ seem to be in best agreement with our experimental results. We did not experimentally observe the strong rotameric preference for C2' *syn* with C4H suggested by Holtje and Marrar's calculations.¹⁵

Our calculations were performed using SPARTAN 2.0 constraining the C4H-C4-C1'-C2' (Figure 2) dihedral angle at 30° increments and optimizing each geometry first with MM2 and then at AM1.²⁷ In the asymmetrically substituted 2'-chloro-6'-methyl-3,5-diester system, **2a**, AM1 calculations predicted a 16.7 kJ/mol rotameric preference for the Cl *anti* to C4H, (*i.e.* disposed over

the DHP ring). The observed rotameric preference (0.9 kJ/mol) is in agreement with this predicted preference though not its magnitude. In the case of the asymmetrically substituted 3,5-dinitrile compound, **2b**, the AM1 calculated preference is 5.0 kJ/mol in favor of the rotamer with the methyl group *anti* to the C4H. This calculated Cl *syn* preference is opposite of that observed and is 2.7 kJ/mol lower in energy than the *anti* form.

In both the diester and dinitrile cases, AM1 predicts the increasing barriers to be in the order 2',6'-dichlorophenyl < 2',4',6'-trimethylphenyl < 2'-chloro-6'-methylphenyl. However, though the order is the same, the calculated $\Delta\Delta H^\ddagger$ values between the dinitriles and diesters are quite different. The calculated barriers for the dinitrile series are, in the 2',4',6'-trimethylphenyl (**1b**) and 2'-chloro-6'-methylphenyl (**2b**) cases, 8.9 kJ/mol higher than the analogous diester compounds. In the 2',6'-dichlorophenyl case, the barrier in the dinitrile compound (**3b**) is calculated to be 11.5 kJ/mol higher than the calculated barrier to in the diester compound (**3a**). Clearly, the halogenation effects and the diester to dinitrile effects are not additive.

Experimental estimates of ΔH^\ddagger were obtained from the Eyring plots and the experimental ΔG^\ddagger values assuming typical ΔS^\ddagger values (see Tables 3 and 4). The computational results (Table 4) are in reasonable accord with the experimentally derived values for ΔH^\ddagger . Two values of ΔS^\ddagger seem to be necessary to describe the data - one for the diesters and a larger one (in absolute value) for the

Table 4. Rotational barrier estimates: AM1 *versus* Experiment

	<u>ΔH^\ddagger (Experimental) (kJ/mol)</u>		
	AM1	Eyring	ΔH^\ddagger (ΔG^\ddagger) ^a
1a	45.2	47.7	48.8 (51.9)
1b	54.1	59.3	60.4 (68.3)
2a	47.7	50.0	49.0 (52.2)
2b	56.6	58.7	58.9 (66.8)
3a	42.2	49.7	49.4 (52.4)
3b	53.7	****	59.7 (66.9)

^a ΔH^\ddagger is derived from the ΔG^\ddagger value from the Eyring plot (in parentheses) using a constant value for ΔS^\ddagger of -12 J/K•mol for the diester compounds and -24 J/K•mol for the dinitrile compounds.

dinitriles. When the experimental ΔG^\ddagger is used, ΔH^\ddagger at T_c is derived using an entropy term of -12 J/K•mol for the diesters and -24 J/K•mol for the dinitriles. Therefore, there are three determinations of ΔH^\ddagger for each compound: one is the AM1 calculation, the second is derived from the Eyring plot and the third is derived from the ΔG^\ddagger using a set value of ΔS^\ddagger for each series (-12 J/K•mol for the diesters and -24 J/K•mol for the dinitriles).

Examining first the 3,5-diester compounds, it was noted that the ranking of the compounds based on the three ΔH^\ddagger determinations are different. Though both ΔH^\ddagger determinations based on experimental data predict **1a** to be the lowest, AM1 predicts the barrier for this compound to be intermediate between **2a** and **3a**. AM1 predicts the largest variance in ΔH^\ddagger between compounds. The difference between the high and low extremes of ΔH^\ddagger by AM1 is 5.5 kJ/mol. Conversely, the ΔH^\ddagger 's from the Eyring plot show an extreme variance of 2.3 kJ/mol and only 0.6 kJ/mol for the constant entropy derived ΔH^\ddagger .

An analogous comparison of the dinitrile compounds gives the following results. AM1 predicts **1b** to have a barrier that is 0.4 kJ/mol higher than **3b**. The experimental data reveal an increase in the barrier of 1.4 kJ/mol in going from **1b** to **3b**. The constant entropy derived ΔH^\ddagger shows this same difference to be only 0.7 kJ/mol with **3b** higher in energy. The lowest experimental ΔH^\ddagger is for **2b** which is 0.1 kJ/mol lower than **3b**. However, the asymmetrically substituted compound has a computationally predicted barrier of 2.9 kJ/mol higher than **3b**. The extreme ranges for the dinitrile series are, at AM1, 2.9 kJ/mol, from the Eyring plot, 0.6 kJ/mol and from the constant entropy derived ΔH^\ddagger , 1.5 kJ/mol.

The effect of the diester to nitrile change is a better determined quantity. The AM1 calculations predict $\Delta\Delta H^\ddagger = 9$ kJ/mol for compounds with a 6'-methyl substituent and 11.5 kJ/mol for the 2',6'-dichloro system. The $\Delta\Delta H^\ddagger$ from the Eyring plots are 12 and 9 kJ/mol, respectively. Those obtained from the experimental $\Delta\Delta G^\ddagger$ values and constant ΔS^\ddagger estimates are more uniform at 10.6 (± 0.7) kJ/mol. Overall, the magnitude of the ester to nitrile mutation is well-modeled by the AM1 calculations though specific experimental trends may not be.

Solid and Solution State Conformational Comparisons

Of all of the methods used for molecular conformational analysis, none has been more widely applied to the dihydropyridines than solid state X-ray analysis. This is, at least in part, due to the fact that the 4-aryl-1,4-dihydropyridines are, with a few notable exceptions, easy to crystallize. The literature is rich with X-ray structures for this series of compounds and some attempts have been made to relate features of the solid state structures with biological activity and/or potency. The most notable of these attempts was made in 1982 by Fossheim *et al.* who noticed a correlation between the planarity of the DHP ring (as defined by the sum of the absolute values of the six internal torsion angles of the DHP ring) and biological activity as a calcium channel antagonist.¹⁰ This report states that the biological activity increases as the DHP ring becomes increasingly planar. There has been at least one published note of a possible exception to this observation²⁸ and it is worthwhile to reiterate that the planar pyridine analogs are devoid of calcium channel blocking activity.

There are also two other general trends that seem to hold for the X-ray structures of DHP's. These are: 1) the DHP ring adopts a flattened boat conformation, and 2) the 4-aryl group tends toward a pseudo-axial orientation on the DHP ring and the 4-aryl ring plane nearly bisects the plane of the DHP ring.

The X-ray structures for five of the six compounds presented in this study are reported in elsewhere.²¹ The structures of **1a/b**, **2a/b** and **3a** were determined. We were unable to obtain x-ray quality crystals of **3b**. Nothing out of the reported norm was noted in the gross geometries of the X-ray crystal structures of the five molecules. However, there exists a finer point with regard to rotameric preference in the asymmetric 2'-chloro-6'-methylphenyl compounds, **2a** and **2b** (Figure 10). Since both have asymmetrically substituted phenyl rings, the possibility for disorder about the ring juncture exists. In fact, both show just that in the solid state. In the case of diester compound **2a**, the refinement indicates a rotameric population distribution of 1:1 in that both the C2'-Cl and

C6'-CH₃ bonds are identical in length (1.684 ± 0.003 Å) and essentially half way between an aromatic carbon - methyl carbon bond (1.531 Å) and an aromatic carbon - chlorine bond (1.759 Å). In contrast, the solution state data indicates a 1.5-1.7:1 ratio of rotamers, most likely due to solvent interactions with the chlorine in the solution state; no evidence of intermolecular contacts to the chlorine exists in the crystal lattice.

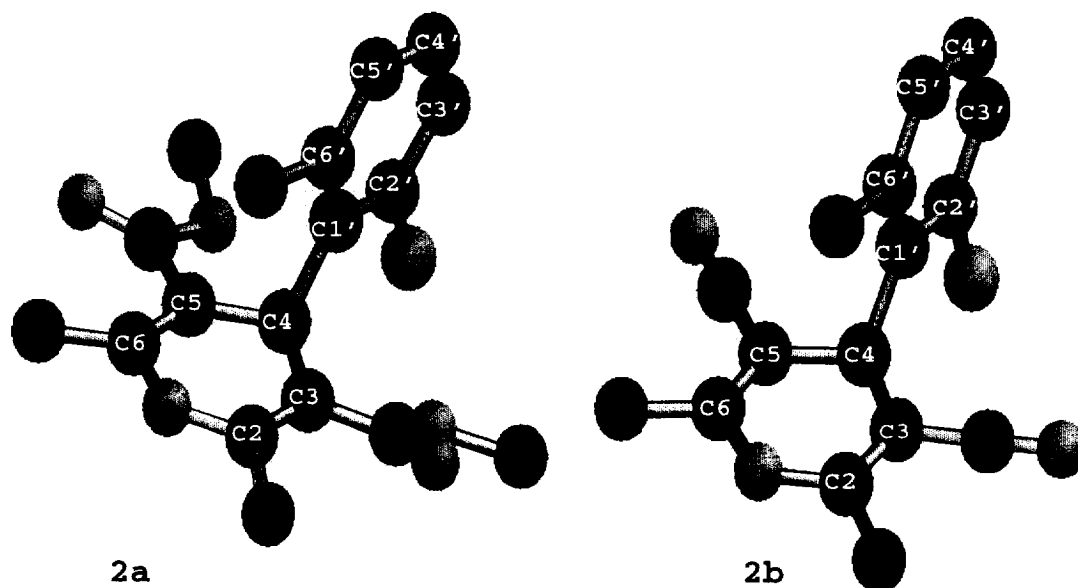


Figure 10. X-ray Crystal Structures of 2a and 2b.

The analysis of the X-ray structural data for the asymmetric dinitrile compound, 2b, was more complicated. When the structure was refined with the 2'-chlorine *anti* to the C4H 100% of the time, the crystallographic R was 0.146. Fits of the data using this rotameric configuration were always poor in that there was insufficient electron density at the 6'-methyl in the refinement to account for the observed diffraction. An improvement in R (to 0.087) was obtained when the structure was refined for a 100% population with the 2'-chlorine *syn* to C4H. Furthermore, the bond lengths in the solved structure were 1.631 Å for the substituent *anti* to C4H and 1.730 Å for the *syn* substituent, after further refinement as described below. Clearly, there is rotational disorder about the C4-C1' bond.

In the ultimate refinement, the bond lengths of the 2'/6' substituents and their fractional populations were allowed to vary. The R value minimized to 0.062 with a 0.74 2'-Cl population and a 1.34 6'-carbon population and the previously stated intermediate bond lengths. The electron density related populations provide the best estimate of the rotameric distribution. To solve for the fractions of each rotamer, the parameter f_{syn} was defined as the rotameric fraction with the chlorine *syn* to the C4H. The following two equations were then solved for f_{syn} .

$$16(f_{syn}) + 6(1 - f_{syn}) = 0.74(16) \quad (2)$$

$$f_{syn} = 0.58$$

$$16(1 - f_{syn}) + 6(f_{syn}) = 1.34(6) \quad (3)$$

$$f_{syn} = 0.80$$

The rotameric distribution is, thus, reported as $69 \pm 11\%$ Cl *syn* to C4H. Recall that the solution state shows a mixture of rotamers with a 4:1 population ratio of the chlorine *anti:syn* to C4H - in clear contradistinction to the solid state data.

Conclusion

We have quantitated the rotational dynamics of a series of 4-aryl-1,4-dihydropyridines in the solution state. Rotameric equilibria of symmetrically and asymmetrically substituted systems were experimentally and computationally compared and the relative rotameric populations rationalized. We have firmly established that in order to experimentally observe the freezing out of C4-C1' bond rotation in the ^1H NMR's of phenyl DHP's, it is necessary to have bulky substituents in both positions 2' and 6'. Furthermore, in compounds with identically substituted phenyl rings in which one had 3,5-diesters and the other had 3,5-dinitriles, the barrier to C4-C1' bond rotation was always higher in the dinitrile case.

Instrumental Methods

^1H NMR spectra were recorded (16K time domain points) on a Bruker AMX500 spectrometer with a sweepwidth of 6024 Hz equipped with an Aspect 3000 computer. Data transformations and analyses were performed on a Silicon Graphics (Personal IRIS) 4D/25TG using FELIX 2.0 (Hare Research, Woodinville, WA). Chemical shifts are reported in ppm downfield from internal $(\text{CH}_3)_4\text{Si}$. All NMR spectra were recorded in "100%" CDCl_3 containing 0.03% (v/v) $(\text{CH}_3)_4\text{Si}$ (Cambridge Isotope Laboratories, Woburn, MA). Typical sample concentrations were 20-30 mM. For the variable temperature experiments, the probe was cooled using liquid N_2 and allowed to equilibrate for 15 minutes at each temperature before each acquisition. All temperatures were corrected using a CH_3OH standard. Solubility, particularly of the 3,5-dinitrile compounds, was notably diminished at the low temperature extremes.

The estimates of rotational barriers were based on equation (1) where $\Delta\nu$ is the chemical shift difference between the individual rotameric signals and T_c is the temperature of coalescence; this equation assumes equal populations of rotamers.²³

$$\Delta G^\ddagger = 19.14 T_c (9.97 + \log(T_c/\Delta\nu)) \quad \text{J/mole} \quad (1)$$

Transient (selective inversion) ΔNOE spectra were collected directly into memory using the pulse sequence described by Andersen *et al.*²⁴ Typically, experiments

$$\text{PD} - ^s180(t_1)_{\text{on/off}} - \tau - ^n90 - t_2 (\text{Acquire}) \quad (2)$$

with 8 'on' and 'off' resonance scans per difference cycle, were parameterized with a preparatory delay (PD) of 1.0 s, an NOE buildup time (τ) incrementally varied from 75-3000 ms and a t_2 acquisition time of 2.05 s. The time t_1 for a selective 180° decoupler pulse was 30 - 45 ms. A $9.5 \mu\text{s}$

non-selective read pulse was employed. A typical NOE experiment collected 16 difference cycles for each value of τ .

X-ray crystal structures of **2a** and **2b** were acquired using the same methods and apparatus reported by Rovnyak *et al.*²⁹ Crystal structure coordinates are available from the authors upon request.

Acknowledgements

The authors would like to thank Dr. Jack Gougoutas, Mr. John DiMarco and Ms. Mary F. Malley for performing the X-ray diffraction study of **2a** and **2b** and providing access to the wealth of dihydropyridine crystal structures determined at Bristol-Myers-Squibb and Dr. S. David Kimball of Bristol-Myers-Squibb for providing compounds **1b** and **3a**. This work was supported by a grant from Bristol-Myers-Squibb, Princeton, NJ.

References

- ¹ Goodman and Gilman's *The Pharmacological Basis of Therapeutics*, 8th edition; Gilman, A. G.; Rall, T. W.; Nies, A. S.; Taylor, P., Eds.; Pergamon Press, Inc.: Elmsford, New York, 1990; p 774.
- ² Loev, B.; Goodman, M. M.; Snader, K. M.; Tedeschi, R.; Macko, E. *J. Med. Chem.* **1974**, *17*, 956.
- ³ Rodenkirchen, R.; Bayer, R.; Steiner, R.; Bossert, F.; Meyer, H.; Moller, E. *Arch. Pharm. (Weinheim, Ger.)* **1979**, *310*, 69.
- ⁴ Janis, R. A.; Triggle, D. J. *J. Med. Chem.* **1983**, *26*, 775.
- ⁵ Miyamae, A.; Koda, S.; Morimoto, Y. *Chem. Pharm. Bull.* **1986**, *34*, 3071.
- ⁶ Mahmoudian, M.; Richards, W. G.; *J. Chem. Soc., Chem. Commun.* **1986**, 739.
- ⁷ Berntsson, P.; Carter, R. E. *Acta Pharm. Suec.* **1981**, *18*, 221.
- ⁸ Gaggelli, E.; Marchettini, N.; Valensin, G. *J. Chem. Soc. Perkin Trans. II* **1987**, 1707.
- ⁹ Triggle, A.M.; Shefter, E.; Triggle, D. J. *J. Med. Chem.* **1980**, *23*, 1442.
- ¹⁰ Fossheim, R.; Svarteng, K.; Mostad, A.; Romming, C.; Shefter, E.; Triggle, D. J. *J. Med. Chem.* **1982**, *25*, 126.
- ¹¹ Fossheim, R. *Acta Chem. Scand.* **1985**, *39*, 785.
- ¹² Fossheim, R. *Acta Chem. Scand.* **1986**, *40*, 776.
- ¹³ Fonesca, I.; Martinez-Carrera, S.; Garcia-Blanco, S.; *Acta Crystallogr., Sect C: Crystal Struct. Commun.* **1986**, *C42*, 1792.
- ¹⁴ Rovnyak, G.; Andersen, N.; Gougoutas, J.; Hedberg, A.; Kimball, S. D.; Malley, M.; Moreland, S.; Porubcan, M.; Pudzianowski, A. *J. Med. Chem.* **1988**, *31*, 936.
- ¹⁵ Holtje, H. D.; Marrar, S. J. *J. Comput. Aided Mol. Des.* **1987**, *1*, 23.
- ¹⁶ Tury Nagy, L.; Jergolova, M. *Chem. Papers* **1989**, *43*, 279.

- 17 Rovnyak, G.; Andersen, N.; Gougoutas, J.; Hedberg, A.; Kimball, S. D.; Malley, M.; Moreland, S.; Porubcan, M.; Pudzianowski, A. *J. Med. Chem.* **1991**, 34, 2521.
- 18 Goldmann, S.; Geiger, W. *Angew Chem., Int. Ed. Engl.* **1984**, 23, 301.
- 19 Coburn, R. A.; Wierzba, M.; Suto, M. J.; Solo, A. J.; Triggle, A. M.; Triggle, D. J. *J. Med. Chem.* **1988**, 31, 2103.
- 20 Loev, B.; Snader, K. M. *J. Org. Chem.* **1965**, 30, 1914.
- 21 Palmer, R. B. *Conformational Studies of Dihydropyridine Calcium Channel Antagonists*, University of Washington, **1994**.
- 22 Palmer, R. B.; Andersen, N. H. *Conformational Dynamics of 4-Aryl-1,4-Dihydropyridine Calcium Channel Antagonists. 2. Computational and Spectroscopic Studies of Possible Dihydropyridine Ring Conformers*, Manuscript in Preparation.
- 23 Gunther, H. *NMR Spectroscopy: An Introduction*; John Wiley and Sons: New York, 1980; p 243.
- 24 Andersen, N. H.; Nguyen, K. T.; Eaton, H. L. *J. Mag. Reson.* **1985**, 63, 365.
- 25 Binsch, G.; Kessler, H. *Angew. Chem. Int. Ed. Engl.* **1980**, 19, 411.
- 26 Natale, N. R.; Triggle, D. J.; Palmer, R. B.; Lefler, B. J.; Edwards, W. D. *J. Med. Chem.* **1990**, 33, 2255.
- 27 Dewar, M. J. S.; Ziebis, E. G.; Healey, E. F.; Stewart, J. J. P. *J. Am. Chem. Soc.* **1985**, 107, 3902.
- 28 McKenna, J. I.; Schlicksupp, L.; Natale, N. R.; Willett, R. D.; Maryanoff, B. E.; Flaim, S. F., *J. Med. Chem.* **1988**, 31, 473.
- 29 Rovnyak, G. C.; Kimball, S. D.; Beyer, B.; Cucinotta, G.; DiMarco, J. D.; Gougoutas, J.; Hedberg, A.; Malley, M.; McCarthy, J. P.; Zhang, R.; Moreland, S. *J. Med. Chem.* **1995**, 38, 119.

(Received in USA 15 April 1996; accepted 22 May 1996)